Reliability Engineering and System Safety 95 (2010) 323–336

Contents lists available at ScienceDirect

Reliability Engineering and System Safety

journal homepage: www.elsevier.com/locate/ress

Performance assessment of topologically diverse power systems subjected to hurricane events

James Winkler [a], Leonardo Dueñas-Osorio [a,*], Robert Stein [b], Devika Subramanian [c,d]

[a] Rice University, Department of Civil and Environmental Engineering, 6100 Main Street, Houston, TX 77005, USA
[b] Rice University, Department of Political Science, 6100 Main Street, Houston, TX 77005, USA
[c] Rice University, Department of Computer Science, 6100 Main Street, Houston, TX 77005, USA
[d] Rice University, Department of Electrical Engineering, 6100 Main Street, Houston, TX 77005, USA

ARTICLE INFO

Article history:
Received 22 July 2009
Received in revised form
7 September 2009
Accepted 2 November 2009
Available online 10 November 2009

Keywords:
Hurricanes
Electrical network reliability
Outage prediction
Topological analysis
Power transmission systems
Power distribution systems

ABSTRACT

Large tropical cyclones cause severe damage to major cities along the United States Gulf Coast annually. A diverse collection of engineering and statistical models are currently used to estimate the geographical distribution of power outage probabilities stemming from these hurricanes to aid in storm preparedness and recovery efforts. Graph theoretic studies of power networks have separately attempted to link abstract network topology to transmission and distribution system reliability. However, few works have employed both techniques to unravel the intimate connection between network damage arising from storms, topology, and system reliability. This investigation presents a new methodology combining hurricane damage predictions and topological assessment to characterize the impact of hurricanes upon power system reliability. Component fragility models are applied to predict failure probability for individual transmission and distribution power network elements simultaneously. The damage model is calibrated using power network component failure data for Harris County, TX, USA caused by Hurricane Ike in September of 2008, resulting in a mean outage prediction error of 15.59% and low standard deviation. Simulated hurricane events are then applied to measure the hurricane reliability of three topologically distinct transmission networks. The rate of system performance decline is shown to depend on their topological structure. Reliability is found to correlate directly with topological features, such as network meshedness, centrality, and clustering, and the compact irregular ring mesh topology is identified as particularly favorable, which can influence regional lifeline policy for retrofit and hardening activities to withstand hurricane events.

1. Introduction

The Gulf Coast of the United States and other hurricane-prone areas suffer from yearly economic, social, and physical disruptions as a result of hurricane events. Of particular concern is the failure of utility systems such as electricity, water, and telecommunications in the aftermath of a hurricane, as most other services rely on the integrity of these lifeline systems to function. The reliability and rapid restoration of the electric grid in particular is necessary to support the needs of the population within the disaster area effectively. Electrical outages are tied to hurricane intensity, network design, local environment, and a host of other factors; an adequate model of outages must therefore account for key aspects of hurricane-related network damage. The outage model could be employed to evaluate the effect of network alterations on system reliability in order to create a direct linkage between reliability and topology. Different types of models exist for the prediction of outages but few have examined the effect of network topology on system performance and reliability when subject to hurricane hazards.

Electrical network damage simulators typically perform one of the following three functions: generating estimates of network reliability, statistically modeling electrical outages, and analyzing topological features of power networks. Models fulfilling the first function use parameter estimation techniques such as Poisson regression to calculate model reliability parameters from historical failure data [1]. These models focus on how network component failure rates propagate to network reliability indices such as system or momentary average interruption frequency indices (SAIFI or MAIFI) [2–4] as affected by wind downbursts, lightning, and vegetation over significant time spans [5–8]. In addition, component based modeling has been used to evaluate the reliability of power networks subject to seismic events [9,10], but other models of this type generally do not evaluate damage on

* Corresponding author. Tel.: +1 713 348 5292; fax: +1 713 348 5268.
E-mail addresses: jwinkler@rice.edu (J. Winkler), leonardo.duenas-osorio@rice.edu (L. Dueñas-Osorio), stein@rice.edu (R. Stein), devika@rice.edu (D. Subramanian).

0951-8320/$ - see front matter © 2009 Elsevier Ltd. All rights reserved.
doi:10.1016/j.ress.2009.11.002

a component level for hurricane events. Given the significant differences between hurricane and seismic hazards, a new component based model is necessary to assess the impact of hurricane hazards upon power network infrastructure.

Statistical outage models utilizing historical spatial outage count and reliability data have been developed to predict regional power outages arising from hurricane events and other storms, along with physical data and environmental conditions of the system component sites [11–13]. Statistical models employ ordinary Poisson regression or generalized linear models [14] to determine outage model parameter estimates. This approach generates accurate outage predictions for discrete sections of a region given additional information concerning terrain, soil type, vegetation, and statistics of network equipment at fine grid size levels. Explicit representation of the power network for topological or flow analysis in this model type is not required, as variables of interest are converted directly into outage counts using the statistical model. While this approach effectively predicts regional outages due to individual hurricanes, no predictions can be made concerning component damage and their impact at the network level.

Analysis of electric transmission network topology[1] is used extensively to identify layout features linked to topological network reliability [15–20]. Pertinent topological properties of electrical and other infrastructure networks [21–23] include network centralization [24,25], and node degree or edge (link) distributions between network elements to identify critical components and cascade susceptibility [20,26,27]. The concept of network damage resistance is explored using these notions coupled with methods that subject network elements to random, targeted, and other types of attack [16,18–20,28,29]. Few if any purely topological models consider local hurricane intensity, terrain, vegetation, or other spatial factors affecting network component fragility. A model connecting network topology to system reliability must incorporate these local network element and environmental properties to accurately assess the impact of hurricane events on the system.

This work applies a proposed joint transmission and distribution component fragility damage model to study how network topology affects the reliability of the power transmission system when subjected to hurricane events. Basic properties including number of substations, generators, and edges along with spatial configurations for six Texas power transmission networks are introduced in Section 2. The component based damage model is developed in Section 3, including the model algorithm, individual fragility models, and model validation at the transmission and distribution levels. The topologies of the previously introduced power transmission networks are explored in Section 4. Hurricane damage responses of the three topologically distinct Bexar, Cameron, and Harris power transmission networks reveal that network performance improves as topology tends towards a compact irregular ring mesh topology, where a substation ring links cliques of substations that interconnect across the network. Finally, the major conclusions of this work are presented in Section 5 concerning the combined use of damage modeling and topological analysis. Select nomenclature is listed in the appendix in Table A1.

2. Electrical network definition

Let G represent an annotated, simple, and undirected graph with vertex (node) set V and edge set E connecting nodes such that $G=(V,E)$ [30]. Each vertex in V represents a power plant, substation, or distribution load point, while each edge in E is a transmission or distribution line connecting vertices without considering edge repetitions. The State of Texas single line power *transmission* system data are obtained from Platts [31]. Power systems are composed of high voltage (230–345 kV) transmission-level networks and low voltage (0.12–35 kV) distribution-level grids [31,32]. The actual electric *distribution* network is not available for analysis due to security concerns; hence, an idealized electric distribution network is synthesized from the local road network information as an alternative [33]. Each intersection of the road network is converted into a distribution load point that is connected to the nearest transmission substation. This approximation faithfully represents the spatial pattern of distribution load (consumption) points, as "distribution circuits are found along most secondary roads and streets" [32] to provide urban and suburban populations with electric service, allow access for construction or repair purposes, minimize the visual impact of overhead equipment by running parallel to existing roadways, and conform to the existing rectangular road grid [32,34]. Local variations in distribution network structure are not discernible using this approach, so the use of the actual distribution network topology is preferred if available. The synthetic distribution network nonetheless matches the essential spatial distribution and topological structure of an actual power distribution network.

The basic composition of transmission networks of six Texas Counties which contain major metropolitan areas are listed in Table 1, including the order or number of generators (power plants) and substations, and the size or number of substation–substation and substation–generator edges (transmission lines) for each network.[2] The average edge length is computed solely from substation–substation edges as the length of substation–generator edges is not available within the utilized dataset. Specifically, the total and average transmission line length ($\widehat{L}$) defined as $\widehat{L}$ = total edge length/number of substation-substation edges are reported for each network. The average substation degree ($\langle k\rangle$) is also computed as $\langle k\rangle = 2$ (number of subtation edges/number of substations) [30]. Generators are counted separately from substations to provide an idea of the differences in electrical generation capacity of the networks. The regions chosen contain several of the largest metropolitan areas in the State of Texas including Houston (Harris), San Antonio (Bexar), Dallas–Fort Worth (Dallas and Tarrant), Austin (Travis), El Paso (El Paso), and Brownsville (Cameron). Although topological properties are reported for the six networks, only Bexar, Cameron, and Harris are chosen for detailed joint topology–hurricane interaction studies due to their larger degree of dissimilarity. While only topological properties of the transmission networks are considered, the properties of the combined power distribution and transmission network could be evaluated as well if the actual distribution level topology is available. This table highlights that transmission networks in sparsely populated areas such as El Paso and Brownsville have much longer transmission lines on average than the more densely populated counties. Generation capacity is more concentrated in counties with denser power substation and transmission infrastructure. Note that the average substation degree is in good agreement with previous studies of power systems across multiple states [36,37]. Geographical representations of all transmission networks are introduced in Figs. 1–3. All networks

[1] Distribution level network topology is typically not available.

[2] Fundamental topological properties conform with definitions in the fields of graph theory and network science [35,36].

Table 1
Compositions of select Texas power transmission networks.

County	Order ($\|V\|$)	Size ($\|E\|$)	Generators	Substations	$\langle k \rangle$	Substation-substation edges	Total edge length (km)	$\hat{L}$ (km)
Harris	463	652	56	407	2.93	596	2 350	3.94
Dallas–Tarrant	445	641	22	423	2.93	619	2 495	4.03
Bexar	298	389	16	282	2.65	373	1 805	4.84
Travis	104	148	15	89	2.98	133	732	5.50
El Paso	74	107	10	64	3.03	97	866	8.93
Cameron	51	68	6	45	2.75	62	631	10.18

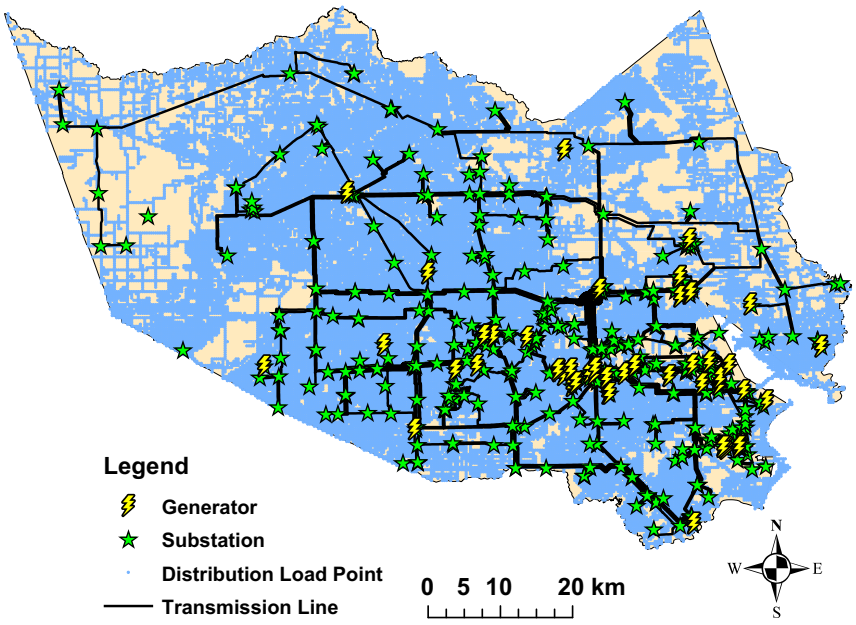

Fig. 1. Harris County power transmission and distribution network.

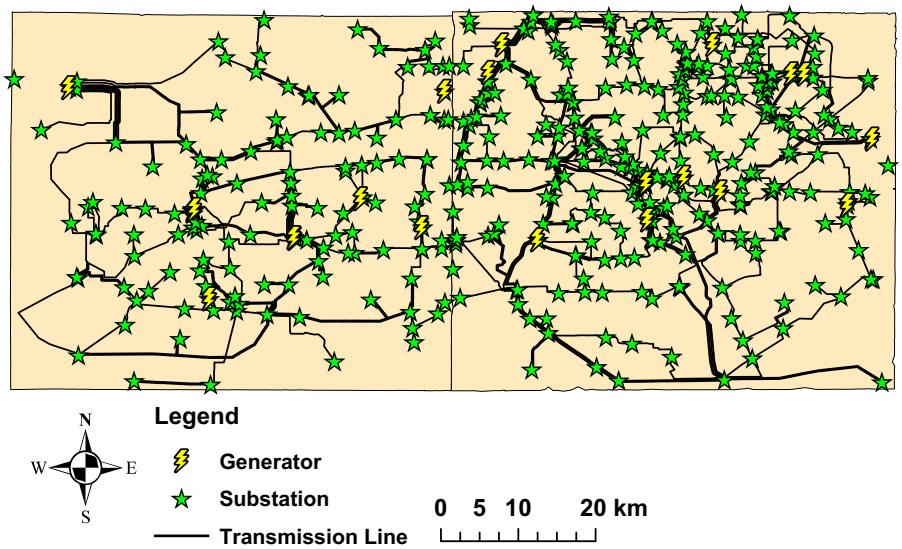

Fig. 2. Dallas–Tarrant power transmission network.

appear topologically unique and should exhibit varied responses to hurricane hazards, even if all were in coastal areas. Several isolated generators and substations are located within each network to supply power to industrial customers or other large consumers. The influence of topological properties on network response to hurricane events is unknown. An approach combining

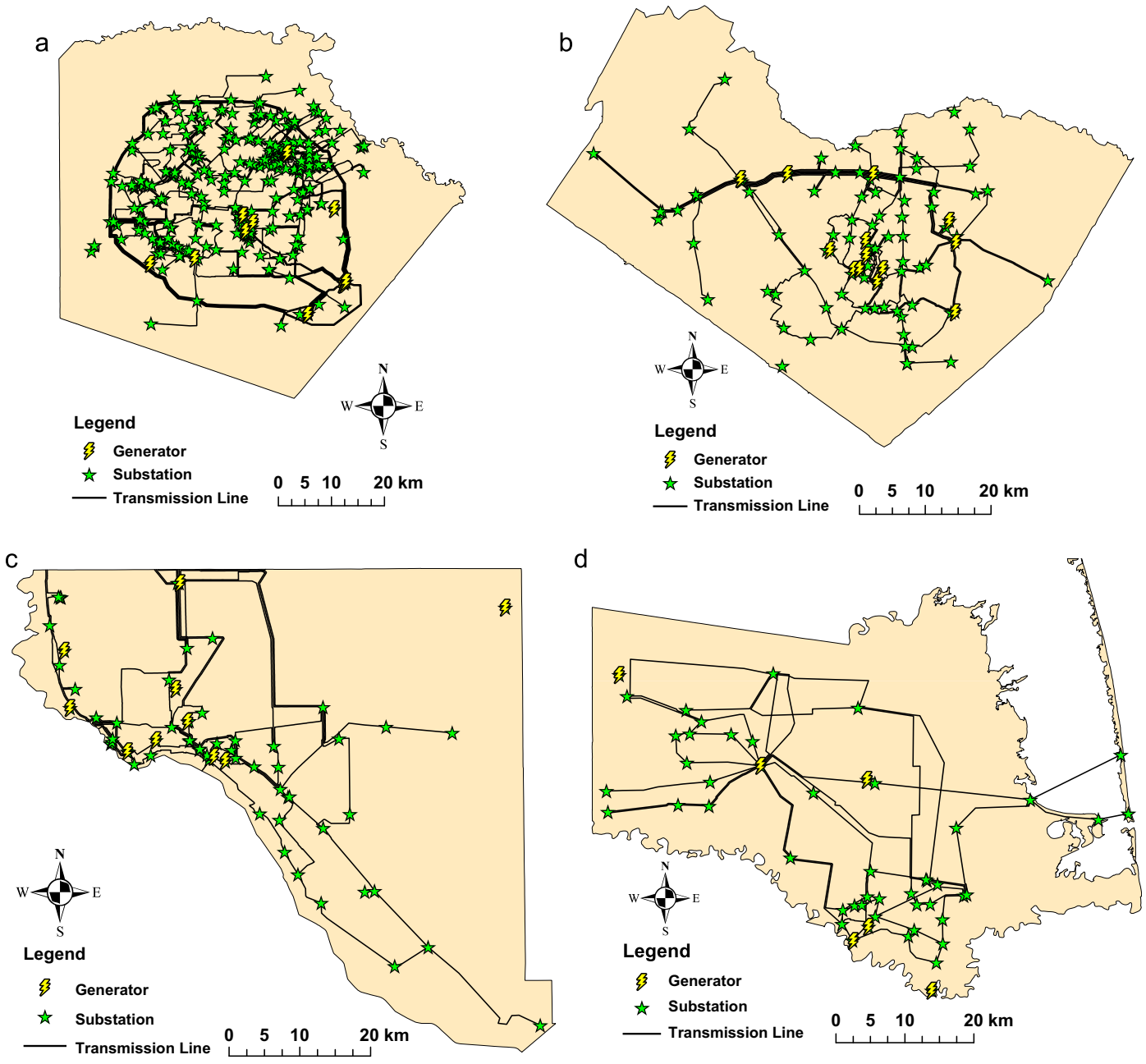

Fig. 3. Additional Texas County power transmission networks. (a) Bexar County. (b) Travis County. (c) El Paso County. (d) Cameron County.

both physical and topological analysis is therefore required to predict electrical grid hurricane damage.

3. Power system damage model definition

The proposed electrical reliability model utilizes the most significant network damage predictors found by Han et al. [13] in their statistical analysis of outages: local terrain and wind speed (3-s gust). In this work, all lines connecting substations to distribution load points and other substations are assumed to be above ground as underground lines are an exceedingly small fraction of utility inventories, though approximately 1/3 of customer connections are underground [38]. The majority of electrical grid failures occur in the distribution system due to the fallen trees and other debris [11]. At the transmission level, wind related damage is expected to be minimal at wind speeds less than $34\,\mathrm{m\,s^{-1}}$, due to structural characteristics and engineered design of substations and transmission lines [39,40]. Damage to a power network element is assumed to cause total failure of the element. Common source events, such as severe storms over the region of interest are taken into account. Power plants are mostly impervious to structural hurricane damage and as a result their fragility is not considered. The proposed model does not include the effects of transient backup generation capacity used to mitigate outages for vital infrastructure. Each element of G therefore has annotations detailing connectivity, local terrain features, physical characteristics, and wind hazard intensity at the site. Distribution load points have a single connection from the point of use to the nearest substation. The

fragility of each component is determined entirely from these parameters, allowing the assessment of power transmission and distribution network damage probability due to hurricane events.

Damage caused by Hurricane Ike to the Harris County electrical network is used for model calibration; however, the modeling approach is applicable to any region of interest. Harris County land cover data is obtained from the Multi-Resolution Land Characteristics Consortium [12,41]. All of the hurricane wind fields are probabilistically generated using HAZUS-MH 3 [42,43]. The specific Hurricane Ike HAZUS scenario for Harris County is provided by the Hurricane Evacuation (HURREVAC) center [44]. Other hurricane models should yield comparable wind fields [45–47]. Simulated wind gusts are generated on a census tract level of granularity, so that each network element is assigned the same wind gust as the host census tract.

All elements in G are associated with a fragility model relating hazard intensity to the probability of structural damage. After the component damage probabilities are computed with the appropriate component fragility model, failures are modeled using Monte Carlo simulation (MCS). The effects of substation or generator failure are added to the direct failure of power demand nodes (distribution load points and substations, along with their incident edges) by automatically propagating disconnection events using the connectivity relationships encoded in G. Following disconnection, the model also monitors in a simple way the temporary cascading power anomalies that can occur in power operation due to abrupt current flow changes. Once failure propagation stabilizes, if a partition of G is completely separated from all generation capacity, an outage is recorded for all nodes in that partition. The outage state of individual components in G is computed for each MCS iteration of the proposed hurricane damage model. Average probabilities of component failure are then determined for each run of N iterations. In this work $N = 50$ for each of several hurricane hazard scenarios considered. Since the hazard and system properties are constant and only component fragilities are random for each 50-trial simulation set, the model standard error per hazard scenario is very low negating the need for the thousands of runs typically required for Monte Carlo models. The disconnection and failure effects of distribution load points are aggregated to the postal (ZIP) code level to compare with the number of outages per ZIP code reported by Centerpoint Energy (serving 2.5 million Harris County residents) immediately following Hurricane Ike [48]. This validation process detailed in Section 3.7 ensures that the model adequately represents damage to network transmission and distribution components so that the same framework may be applied to other networks. Details of the proposed power system damage model are presented next.

3.1. Power system damage algorithm outline

The proposed model computes the failure probability $p_{f,i}$ of the ith component $\forall i \in V, E$ so that damageable graph elements are tested according to their corresponding component fragility model. The model requires as inputs a graph $G(V, E)$ representing an electrical network, including transmission, distribution, and power linkages, and a list V_{ss} of all unique substations in G. The simulated element failure during each Monte Carlo model iteration is performed by comparing a uniformly distributed random variable $r \in [0, 1]$ to $p_{f,i}$. If $r \leq p_{f,i}$, then the element is assumed to have failed during that model iteration. The components considered, fragility parameters, and model algorithms are detailed in Tables A2 and A3, and Appendix B. The computational cost of analyzing a network with m components (elements) subjected to N model iterations requires a simulation runtime of order $O(Nm)$ operations. Analysis of very large networks is therefore quite feasible. The fragility models of each network element are selected to maximize accuracy while minimizing the number of required parameters. The fragility models available or assumed for each network component are now discussed.

3.2. Substation fragility

The damage probability of substations is represented via log-normal fragility curves. These curves generate the probability of damage for a given wind gust speed (W_s) while taking into account the local terrain and structural characteristics of the substation under consideration. This approach is considered standard for modeling of urban and suburban structural fragility in response to hazard events. The general form of the fragility curves is given as follows:

$$p_{f,SS,i}(\text{Moderate damage}|W_s = x) = \int_x^{-\infty} \frac{1}{\sqrt{2\pi}\sigma} \exp\left(\frac{-(\ln(x) - \mu)^2}{2\sigma^2}\right) dx \tag{1}$$

where $p_{f,SS,i}$ is the ith substation moderate damage probability of exceedance given wind speed x at the substation site, calculated using the fragility curve corresponding to the terrain near the substation (see Algorithm B1, lines 3–5). The parameters μ and σ represent the logarithmic mean and standard deviation of the pertinent fragility curve. Fragility curves for each type of modeled terrain and building type are taken from HAZUS-MH 3 internal data files [49]. This method considers substations as a single unit instead of employing fragility curves for individual substation elements as a first approximation. The selected curves can be updated once more data concerning the structure and vulnerability of substations are available. Substations also fail if not connected to at least one generator node within the cluster containing that substation ($C(v)$) (see Algorithm B2, lines 17–20).

3.3. Distribution load point fragility

Distribution load points are modeled as utility poles. Log-normal cumulative distribution functions relating storm return period (RT) to probability of pole failure are calculated by Gustavsen et al. [50]. This log-normal curve generates the probability of load point failure $p_{f,LP,j}$ for the jth load point and is of the same form as those used for estimating substation damage probability (see Algorithm B1, lines 3–5). It is necessary to convert wind speed (W_s) to the corresponding return period via Eq. (2), derived from HAZUS-MH 3 by correlating hurricane return period to average storm wind speed, to make use of the Gustavsen damage model:

$$RT = 0.2064\mathrm{e}^{(0.05889W_s)} \tag{2}$$

Poles in all regions are assumed to be relatively new, as no data about pole age distributions in the areas under consideration are available. Load points are also assumed to fail if disconnected from the transmission network. Aging effects are readily incorporated into the Gustavsen model if these data become available in the future.

3.4. Power system flow fragility

Power transmission and distribution networks easily re-route power around damaged elements arising from equipment failure or catastrophic events, provided that alternative routes exist and power balance is feasible. The change in power flow through the damaged transmission network is approximated by comparing

betweenness scores of nodes not inactivated by direct damage or disconnection events in both the damaged and the original networks [17,26]; betweenness is a proxy for the amount of current passing through network elements and is related to the number of shortest paths that pass through every node when connecting all supply and demand points. Given that abnormal current events (ACEs) are a transient condition and typically do not result in permanent equipment damage, failures are not recorded for nodes suffering from aberrant power flow conditions. Simply, a node overload or underload is recorded if the change in node betweenness score between the original and damaged network exceeds a certain threshold α to predict power redistribution in hurricane damaged networks (see Algorithm B2, lines 22–26) [15,26]. This work utilizes a value of $\alpha = 0.75$ for all substations as a first approximation [26].

3.5. Transmission and distribution line fragility

The majority of damage suffered by transmission and distribution lines is due to excess wind loading and/or flying debris. Oliver et al. [51] along with other groups have proposed wind downburst models [52] to predict the effect of sudden, hurricane strength winds on both types of lines, but these models focus on the prediction of downburst event occurrences rather than damage to electrical conductors. Tornado downburst models [53] are constructed in much the same way and do not relate the wind intensity directly to line failure fragility.

Given that wind loading is a major cause of line failure, the ratio of the wind force and maximum rated line perpendicular stress resistance will be used to approximate the probability of line failure (see Algorithm B1, lines 6–8). This approach effectively approximates line damage in the absence of more sophisticated models. The wind force on any line k is calculated with the standard American Society of Civil Engineers (ASCE) design equation using wind gust speed squared (W_s^2) and line cross-sectional area A_c:

$$F_{wind} = Qk_zI_{FW}G_{WRF}C_fA_cW_s^2 \tag{3}$$

The other parameters in Eq. (3), meant to account for air density (Q), terrain correction (k_z) hazard importance (I_{FW}), wire strain (G_{WRF}), and drag coefficient (C_f) are defined by the ASCE Engineering Practice Report 113 [39]. Open and light suburban areas are assigned to the Exposure C terrain class, while Exposure B contains all other areas under consideration. All conductors are assumed to have an effective height less than 15 m. The other parameters may be calculated from these assignments. The transmission and distribution lines are assumed to be 'Zebra' and 'Horse' aluminum/steel conductors respectively [40]. Line damage probability is calculated as the simple ratio of the maximum perpendicular force that the line can endure ($F_{brk,k}$) and the line wind loading ($F_{wind,k}$) for transmission or distribution line k:

$$p_{f,wind,k} = \min\left(\gamma\frac{F_{wind,k}(W_s)}{F_{brk,k}}, 1.0\right) \tag{4}$$

The factor γ is used to scale the line fragility estimates to match recorded failure data. The probabilities of transmission ($p_{f,TL,k}$) or distribution ($p_{f,DL,k}$) line failure completely or partially depend on their $p_{f,wind,k}$ values, respectively. Note that at least one other existing model estimates damaged feeder fragility by correlating line fragility to the square of wind gust speed using empirical wind damage data [4].

The distribution network suffers from significant vulnerability to damage caused by flying debris, as the distribution lines are closer to the ground and often in close proximity to significant numbers of trees [38]. Tree windthrow probability therefore affects the fragility of distribution lines significantly. The fragility of the distribution lines may be represented by whichever fragility is greater:

$$p_{f,DL,k} = \max(p_{f,wind,k}, p_{f,FD,k}) \tag{5}$$

where $p_{f,FD,k}$ represents the probability of tree windthrow near distribution line k, as developed in the flying debris fragility model below. Debris effects are not modeled for transmission lines, as vegetation impacts sufficient to disrupt transmission line are comparatively uncommon. The type of tree being thrown is chosen randomly from a set of seven possibilities to reflect the natural heterogeneity of the local tree population.

3.6. Flying debris model

This model focuses on trees that, when damaged by wind, cause damage to overhead distribution lines by falling or otherwise impacting the lines. The predominant model of tree windthrow are species specific logit regressions proposed by Canham et al. [54]. Other types of models are available, including similar logit models [55–58] and widely used HWIND and GALES physical models [59,60]. The Canham model is used here for accuracy and simplicity:

$$\log\left(\frac{\beta p_{f,FD,k}}{1-\beta p_{f,FD,k}}\right) = a_s + c_s(k_zS_k)D_{BH}^{b_s} \tag{6}$$

where $p_{f,FD,k}$ is the failure probability due to flying debris in the vicinity of line k; a_s, b_s, and c_s are species specific constants, S_k the wind intensity (0–1 scale) at the kth distribution line, β a factor for adjusting impact importance, and D_{BH} the tree diameter at breast height (cm). The S_k parameter is generated by dividing the local wind hazard by the maximum wind hazard in the region of interest. The factor k_z adjusts the hazard intensity to account for local terrain effects, including tree density, and is chosen based upon the land cover information near the line [39]. The D_{BH} variable is assumed to be 15 cm as approximately 70% of the tree inventory has a D_{BH} less or equal to 20 cm. Trees in Harris County are also assumed to be uniformly distributed between the seven species for which data are available as a first approximation (see Algorithm B1, lines 6-8) [54].

3.7. Failure prediction optimization and validation

The number of outages from Hurricane Ike for each Harris County ZIP code is obtained from Centerpoint Energy [48]. The actual outage percentage within a ZIP code is calculated by dividing the number of customers without power reported on 9/13/08 (11 AM) by the ZIP code population obtained from the US Census 2000. A total of 137 ZIP codes in Harris County are available for analysis. The proposed joint transmission-distribution fragility model predictions for load point failure are also aggregated to the ZIP code level for validation purposes. In addition, transmission level predictions are sought to match failure rates and causes as published by Quanta Technologies [38].

The absolute model error for the z th ZIP code AE_z is found from the absolute difference between the predicted ZIP code outage ($p_{pred,z}$) and the actual recorded outage rate ($p_{act,z}$) for that ZIP code. The overall mean error of the model $\widehat{ME}$ over Z ZIP codes is calculated using Eq. (7). Use of the absolute or mean square model error will give similar results; $\widehat{ME}$ is guaranteed to be larger than the mean square error, however, providing an upper bound on the model uncertainty:

$$\widehat{ME} = (1/Z)\sum_{z=1}^{Z} AE_z \tag{7}$$

A search of the conductor scaling parameter space $\beta, \gamma \in [0, 1]$ may be performed to find values for β and γ that minimize $\widehat{ME}$. The

calibration ensures that the methodology is readily applicable to other Gulf Coast hurricane scenarios.

3.8. Simulator results

Fifty simulations of electrical grid damage caused by Hurricane Ike are used to test the coupled power transmission-distribution damage model. After optimization, the average ZIP code outage prediction error is $\widehat{ME} = 15.59\%$ with a standard error of $\sigma_e = 0.02\%$. The errors of 98 out of 137 available ZIP codes are less than or equal to $\widehat{ME}$. The geographical distribution of these errors is given in Fig. 4. These model errors arise from assumptions made for component fragilities and anomalies in the validation data, as the number of affected customers recorded in several ZIP codes exceeded the ZIP code population. The inclusion of substation and line equipment vulnerable to hurricane damage along with the effects of backup generation capacity and private retrofits to power systems (as is the case in downtown Houston complexes and the Texas Medical Center area—yellow to orange in the central part of Fig. 4) may also improve the accuracy of the simulation. Even with these errors, the joint transmission/distribution physical damage model approach effectively captures the essential pattern of expected outages when compared to the actual damage distribution.

Predictions for only the Harris County power transmission network fragility are shown in Fig. 5. A closer look at these transmission systems is relevant because the transmission grid

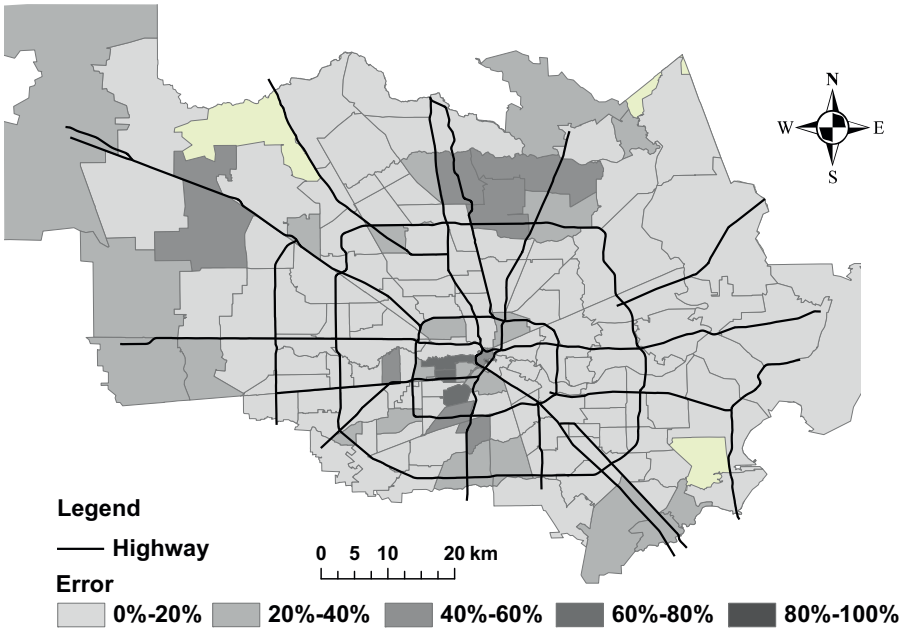

Fig. 4. Outage prediction error distribution for hurricane Ike damage in Harris County.

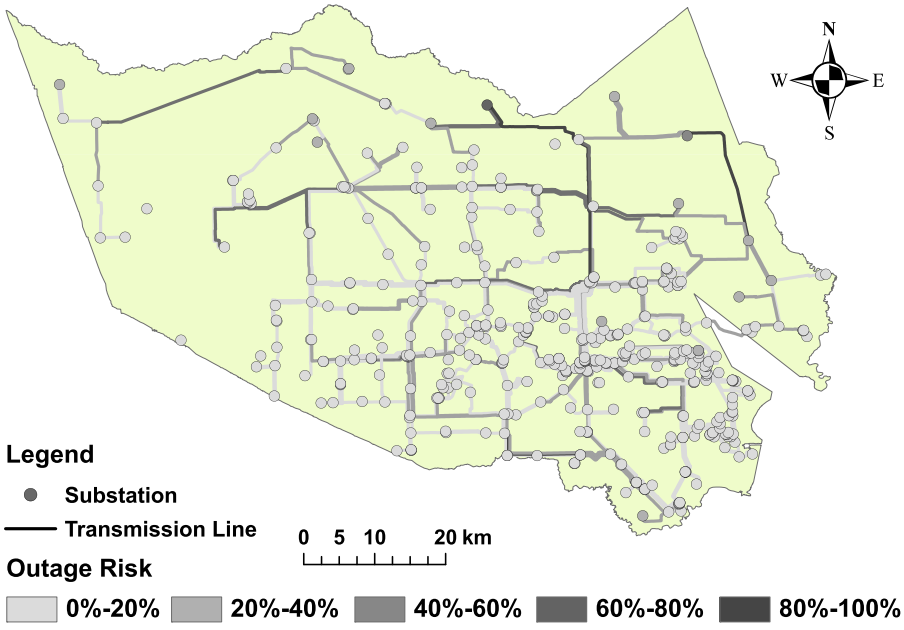

Fig. 5. Predicted hurricane Ike-related transmission grid damage.

routes power to the distribution network and to interdependent systems so that any damage at this high level network affects power distribution and other utility networks dependent on steady power supply [61,62]. Transmission level network damage is minor compared to distribution network damage but the pattern of damage closely follows the wind intensity throughout the county. Height, material, and design characteristics explain the low overall damage incurred by the transmission network elements. The predicted average damage probabilities for substations ($\widehat{p}_{f,SS,p}$) and transmission lines ($\widehat{p}_{f,TL,p}$) determined by averaging over the 50 simulations ($\widehat{p}_{f,SS,p}=3\%$, $\widehat{p}_{f,TL,p}=9.76\%$) compare favorably with the actual average outage proportions for these two components ($\widehat{p}_{f,SS,a}=5\%$, $\widehat{p}_{f,TL,a}=9.95\%$) recorded by Centerpoint Energy in the aftermath of Hurricane Ike [38]. Transmission network damage is a serious issue at higher wind speeds, given that substation and line fragilities increase exponentially and quadratically (respectively) as a function of wind speed.

These results demonstrate that the proposed model successfully predicts the extent and causes of damage for all components within electrical networks. In addition to outage prediction, the component based approach of the damage model facilitates study of network structural and topological properties influencing overall reliability. Understanding how the topology of a network influences the outage extent caused by hurricane events allows utility managers to strategically introduce modifications to prepare and cope with outage vulnerability.

4. Topological network fragility due to extreme events

The relationship of transmission level network topology to system reliability is sought. Damage to transmission grid components has a significant impact on the service areas and therefore will be the focus of topological analyses, putting aside the distribution network portion of the grids. The developed damage model allows for direct relation of physical fragility and internal connectivity (topology) to remaining network functionality after exposure to hurricanes. Several network topological properties are of particular interest: the number of redundant paths (meshedness), the length of redundant paths (cycle length distribution), and the distribution of edges among nodes (clustering coefficient, centrality, and degree distribution). The formal definitions of these properties are stated in Section 4.1. The influence of these topological properties on remaining network reliability is explored through application of the damage model and a range of simulated hurricanes.

The selected network properties are chosen for their potential ability to predict system response to hurricane damage. The meshedness and cycle length distribution metrics reveal the number and length of alternate paths that exist for current flow redistribution within a given geographically distributed network [21]; more reliable networks should have many short, redundant paths to maximize system uptime. Determining the centrality of each node and the overall network clustering coefficient provides the information to characterize node importance and the distribution of redundant paths within networks at the node neighbors scale. The network element failure probability predictions generated by the damage model at the local level are converted into network performance assessments by assessing changes in the approximated flow of current, and the effect of failed substations on network connectivity through the size of the remaining connected network as functions of wind speed. Since current tends to follow the shortest path available between substations, node overloads and underloads are also measured, since they reflect the abnormal current flow within damaged networks caused by altering the distribution of shortest paths connecting surviving nodes and edges [24–26].

The final element of this topological analysis is a comparison of resistance to hurricane damage and the effects of randomly removing nodes. Rosas-Casals et al. [20] and Cohen et al. [63] quantifies random damage tolerance via the critical fraction of removed nodes p_c to determine when networks decompose into small, unconnected clusters due to node removals. A new hazard based parameter linking topology to reliability under hurricane hazards combining these two concepts of damage resistance is the wind speed at which the network experiences critical failure (W_c): the wind speed where the size of the largest connected component (LCC) of each network contains only a $(1-p_c)$ fraction of nodes in the network. The LCC size of a hurricane damaged network is roughly analogous to the amount of network functionality remaining after a hurricane impact. This approach weights the loss of each node proportionally to its overall spatially dependent fragility within the network by applying the developed physical damage model to individual system elements instead of assuming all nodes are equally damageable [15,20]. The W_c parameter provides a simple, easy to understand measure of network resistance to hurricane damage that incorporates network topological properties. The topological properties and hurricane response of the Bexar, Cameron, and Harris county transmission networks are assessed in order to determine the relationship between topology and system reliability.

4.1. Topological analysis methods

Aspects of network topology that are of particular interest when analyzing the ability of power networks to resist hurricane damage include internal redundancy, network centralization, and network performance. Synthetic networks with the same size as each real transmission network and the maximum number of non-overlapping edges possible in a 2D plane, termed maximally planar graphs (MPG), are used to normalize the topological metrics when appropriate [21]. Network redundancy is the ability of electricity to reach the same destination through multiple paths (nodes and edges between nodes of interest) and significantly affects network tolerance to hurricane damage. The number of these alternative paths (or cycles) is measured using the meshedness coefficient M and is easily calculated via the following equation [21]:

$$M=\frac{|E_{net}|-|V|+1}{|E_{MPG}|-|V|+1} \tag{8}$$

where $|V|$ is the number of nodes in the transmission network, $|E_{net}|$ is the number of edges in the same network, and $|E_{MPG}|$ the number of edges in the maximally planar graph. A larger meshedness coefficient indicates a greater number of faces (cycles) are present within the network.

Cycle length also influences network response to damage, as shorter paths tend to limit propagation of current through damaged networks [21,64]. Proportions of cycles containing 3–5 nodes normalized by MPG results are generated using Eq. (9) for all networks. The proportion of cycles with length k (C_k^*) is computed by raising the adjacency matrix A of the power network to the kth power and taking the trace ($\mathrm{Tr}(\cdot)$) of the resulting matrix. The result is normalized by the number of k-cycles in the corresponding MPG:

$$C_k^*=\frac{\mathrm{Tr}(A_{net}^k)}{\mathrm{Tr}(A_{MPG}^k)} \tag{9}$$

Given the grid-like nature of most infrastructure, cycles of length 4 predominate in real networks. Centralization, the concentration of shortest paths through specific nodes, is another key influence

on network reliability. The parameter $\widehat{B}$ defined in Eq. (10) reflects the proportion of shortest paths passing through nodes with 90th percentile or above betweenness scores (set V_p) to estimate network centralization [24,25]:

$$\widehat{B} = \frac{\sum_{V_p} C_B(v_i \in V_p)}{\sum_{V} C_B(v_i \in V)} \tag{10}$$

where C_B represents the betweenness centrality of node v_i in terms of the number of shortest paths that pass through it. A large $\widehat{B}$ score indicates that a small group of nodes control current flow within a network. Finally, the local edge distribution in a network is explicitly identified by the network clustering coefficient γ_G, representing the proportion of node triplets within each network that are 3-cycles [36] and is calculated here using the UCINET 6 social network analysis software [65].

The collective effects of these topological factors are determined by quantifying network performance in the aftermath of simulated hurricanes. Performance in this work is measured using the size of the largest connected component (LCC) normalized by the LCC of the undamaged network, and using the percent of node betweenness loss. This loss is captured by determining the fraction of node betweenness represented by failed nodes in the undamaged power transmission network. Both LCC and betweenness loss are reported to estimate the remaining level of functionality in hurricane damaged networks as functions of storm average wind gust speed, defined as the average of all census tract wind gust speeds for each region under consideration. Note that individual element failures are calculated with the wind speed at the site of the element. The average wind speed $\widehat{W}_s$, used for reporting purposes, is calculated for each hazard scenario applied to the Bexar, Cameron, and Harris Counties. The performance metrics are computed by averaging the LCC size and betweenness loss predictions generated with the developed damage model over 50 simulations for each hazard scenario under consideration. Given the exponential and quadratic dependence of these performance metrics with $\widehat{W}_s$, a logistic decay function (Eq. (11)) is used to correlate the set of individual LCC size estimates (P_{LCC}) to the average storm wind gust speed. The R^2 value of these correlations is above $R^2 = 0.95$ unless otherwise noted.

$$P_{LCC}(\widehat{W}_s) = \frac{1}{1 + Ae^{-B\widehat{W}_s}} \tag{11}$$

The quantities A and B are network specific regression constants. Large connected component decay rates are derived using the correlations generated from Eq. (11), while network critical wind speeds are generated using the corresponding inverse function. The betweenness loss–wind speed relationship may also be explored using a functional form identical to Eq. (11).

Table 2
Topological properties of power transmission networks.

County	$\widehat{B}$	γ_G	p_c	M	C_3^*	C_4^*	C_5^*
Harris	0.550	0.077	0.658	0.182	0.058	0.146	0.029
Dallas–Tarrant	0.601	0.084	0.674	0.174	0.051	0.133	0.025
Bexar	0.641	0.108	0.393	0.133	0.039	0.158	0.027
Travis	0.490	0.132	0.660	0.231	0.113	0.187	0.063
El Paso	0.473	0.086	0.642	0.186	0.073	0.161	0.042
Cameron	0.507	0.011	0.693	0.165	0.021	0.142	0.013

4.2. Survey of network topological properties

The networks under consideration exhibit noticeable differences in meshedness, cycle length distributions, centralization, clustering, and critical fraction of removable nodes as seen in Table 2. Cycles of length 4 predominate in all networks given the grid-like structure of existing infrastructure as expected [34], though the proportion of 3-cycles in the Travis network is significantly greater than the other networks considered. The Bexar network is the most centralized of the networks and is the least meshed, indicating the presence of fewer redundant cycles than the other networks considered. The high degree of centralization in the Bexar network is due to the majority of redundant paths passing through a subset of spatially distributed and homogeneous critical nodes (V_p) that have the means to connect with each other and non-critical nodes efficiently via shortcuts. The extent of neighbor–neighbor interaction within the Bexar network is quite substantial given the large clustering coefficient which improves local connectivity, although this clustering occurs within small cliques as demonstrated by the low average vertex degree and meshedness of the real topology. This result suggests that the Bexar network will effectively resist large scale failures if hurricane damage does not disable the core of critical nodes that span the network outer ring and inner clusters. In contrast, random node attacks weaken the Bexar network especially due to the significant loss in redundancy that accompanies spatially distributed and homogeneous critical node failures along with their incident edges within the ring or irregular inner mesh. Also, the proportion of nodes in Bexar without null betweenness scores contributing to system connectivity is 35% and 30% less than in Cameron and Harris networks, respectively. Hence, more nodes participate in maintaining the Bexar system functionality, which renders the network more vulnerable to random failures. In comparison, the Cameron network is likely to exhibit a better response to random failures due to a much lower clustering coefficient and lower node centrality concentrated on a few nodes that produce a hub-like transmission topology with some long cycles. This layout is difficult to disintegrate by chance damage. However, hurricane damage to these few hub nodes or long inter-hub links will effectively partition the network due to its small size, lack of redundant transmission lines, and absence of potentially more wind tolerant cliques like those found in the Bexar network. Larger networks such as that of Harris County appear to be midway between these two extremes in their topological metrics. Detailed analysis of network response to hurricane damage is required to determine the relationship between these suggestive properties and system reliability.

The damage responses of the Bexar, Cameron, and Harris networks to simulated hurricane events are considered. These networks have significantly different topological structures and thus provide the best opportunity to determine how topology affects network reliability. Visual inspection of the Bexar network in Fig. 3a reveals a distinct ring pattern where an outer loop of substations transmits power into inner substations using an irregular mesh of redundant connections and to outer substations through radial connections. The comparatively high clustering coefficient of the network supports this observation. The Cameron network in Fig. 3d is several weakly connected stars and lacks local redundancy given the negligible clustering coefficient; the Harris network in Fig. 1 is a mixture of several structures, containing rings, stars, meshes, and tree-like topological arrangements.

Traditional graph theoretic methods for evaluating network reliability focus on random attacks, where nodes within the network are randomly removed consecutively until the network

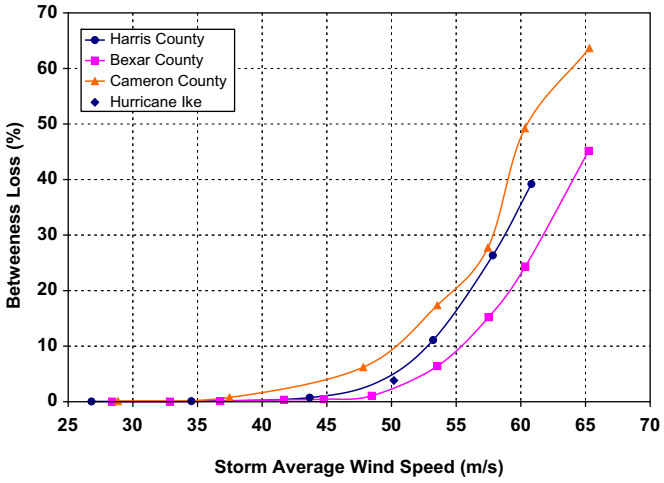

Fig. 6. Betweenness change of transmission networks.

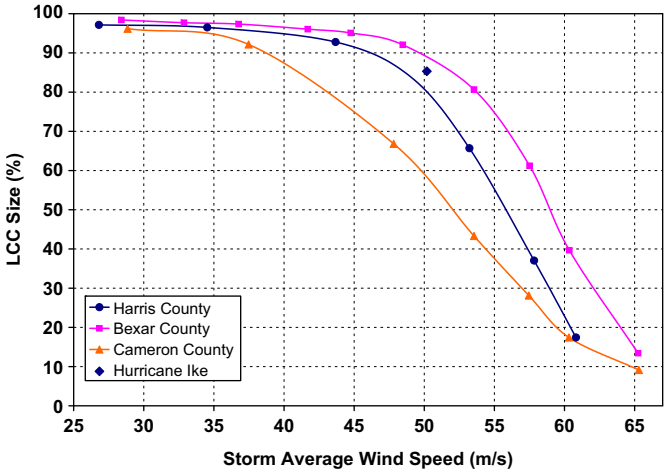

Fig. 7. Normalized size of LCC versus wind speed.

decomposes into small, disjoint partitions. This type of damage resistance has been explored for many types of real and artificial networks [15–17,20]. The p_c scores for each network listed in Table 2 indicate that all networks except that of Bexar County may sustain a loss of approximately 65% of substations while remaining largely connected. The importance of each node within the networks is inversely proportional to the network p_c score; removing substations from networks with low p_c scores and more homogeneous vertex degree increases the average path length between the remaining substations compared to networks with higher p_c scores and less homogeneous vertex degree. Though the network p_c score provides useful insight into the ability of a network to tolerate random damage, hurricanes do not inflict damage in a random fashion. Spatial damage modeling must be employed to ascertain the relationship of these topological properties to hurricane damage response.

4.3. Hurricane damage resistance

The physical damage model is needed to see which topological arrangement best absorbs hurricane winds while maintaining network functionality. Bexar,[3] Cameron, and Harris Counties are exposed to 10–1000 year return period wind fields to predict the impact of these storms on network function. The Hurricane Ike scenario, generating an average storm wind speed of 50 m s^{-1}, is also included for Harris County. The betweenness losses among substations and largest connected component size (LCC) behaviors in Figs. 6–7 reveal an exponential decline in network function as hazard intensity increases. These responses are qualitatively similar to those found for random removal [20] but the use of the damage model ensures that network elements subject to the highest hazard intensity are removed preferentially allowing definitive conclusions to be drawn concerning the comparative performance of network topologies. The Bexar network suffers fewer losses of critical nodes than the other networks, though the removal of important nodes initiates at approximately 48 m s^{-1}. The size of the LCC in each network declines rapidly once a threshold wind speed is exceeded due to increased substation damage. Network function should decline rapidly at high wind speeds for all transmission networks.

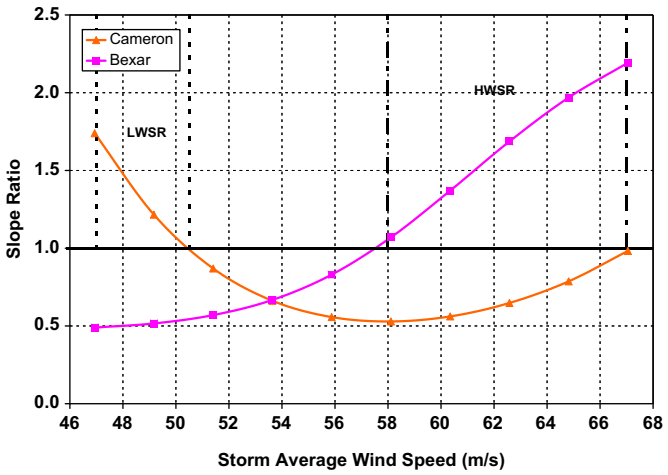

Fig. 8. Normalized rate of LCC size change and wind speed regimes.

The Bexar network performs better than the other networks considered, suggesting that the ring–mesh topology of that network resists wind hazards effectively, despite the fact that random attacks are more likely to affect it. The rate of change in LCC calculated using the Eq. (11) logistic correlation is of particular interest, as the network most vulnerable to disruption should have the most rapid rate of performance decline as wind speed increases. The normalized slopes of each county (relative to Harris County) in Fig. 8 clearly reveal wind speed regimes where the LCC sizes change quite rapidly for each network. Two distinct wind damage regimes are identified at 47–51 (low impact speed wind regime, LSWR) and 58−67 m s^{-1} (high impact speed wind regime, HSWR) by comparing the damage rates for all three networks to that found for Harris County. The extent and rate of network performance loss is therefore a function of the topology of each network.

The Bexar network LCC size decreases more rapidly than other networks at higher wind speeds, while surprisingly the Cameron network LCC size declines rapidly at a lower wind speeds. The additional redundancy afforded by the ring and central irregular mesh of the Bexar network ensure that spatially distributed critical substations remain connected to the network until the wind speed is sufficient to damage the substations themselves.

[3] Wind gust speeds in each Bexar census tract are assumed to be within half a standard deviation of the average wind gust speed of all Harris County tracts at each return period. This approximation is necessary to test the resilience of the Bexar network as it is rarely subject to strong winds.

Table 3
Critical wind speeds.

County	p_c	W_c (m s^{-1})
Bexar	0.393	56.86
Cameron	0.693	59.53
Harris	0.658	57.75

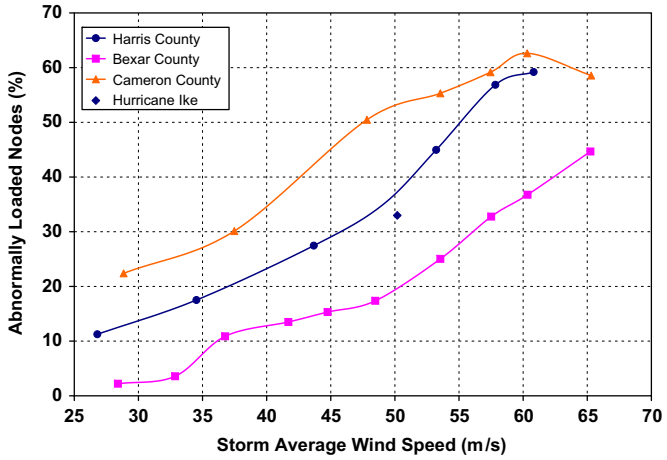

Fig. 9. Network abnormal current flow profiles.

This behavior is preferable as wind gusts above 58 m s^{-1} are rare and less functionality is lost from the Bexar network at lower, more common wind speeds. The especially low local interconnectivity and high centrality of the few Cameron network hubs compared to the other networks may explain the rapid decline of the LCC size at lower wind speeds, as the long edges or weak nodes removed due to relatively low wind speed substantially degrade network connectivity.

The network W_c parameters in Table 3 are surprisingly similar when compared to their associated critical fractions of removed nodes. The Bexar network has only lost approximately 40% of substations once the critical wind speed is achieved compared to the much greater losses of the Cameron and Harris network at a similar wind speed. Ironically, these two Cameron and Harris networks possess a larger proportion of generators among the set of nodes, which may not be able to deliver the flow due to significant damage in the substation and transmission line infrastructure. The respective betweenness losses of the networks in Fig. 6 at their critical wind speeds reveal the network path redistribution ability and the lower centrality of the failed Bexar substations (while the most centralized nodes remain operational); more functionality is therefore retained by the Bexar network at the critical wind speed than the other networks under consideration since less bottlenecks exist (i.e., less potential overload events) for its adequate functionality. Power restoration should occur more rapidly and be less costly in Bexar County due to its compact ring and irregular mesh topology as a result.

To complement the topology-based insights, the abnormal current event count metric provides the means to observe the hurricane impact upon network functionality by observing changes in node betweenness centrality above or below the preestablished threshold α. These changes correspond to alterations in the approximate power flow within damaged transmission networks, though actual power stability analyses must be performed in the future for grid operational insights. The network abnormal current event profiles given in Fig. 9 indicate that both the Cameron and Harris County networks suffer substantially more overloads than the Bexar network at all wind speeds considered.

Though most abnormal power flow conditions are fundamentally transient events that will be cleared automatically by protective equipment, reliable networks have fewer abnormal loads when subjected to external damage. These events at lower wind speeds result from damage to conductors while substation failure becomes the primary trigger for system abnormal load conditions at wind speeds above 48 m s^{-1} for all networks, as significant network betweenness loss is shown to begin at that wind speed in Fig. 6. Changes in node betweenness are better distributed throughout the Bexar network, given the lower fraction of abnormally loaded nodes and due to the greater retention of connectivity and capacity between undamaged and well distributed substations than in the other networks. The Cameron network exhibits the most nodes experiencing abnormal power flow events due to the previously identified lack of redundancy.

The Bexar transmission network is most able to resist the effects of hurricane damage according to all performance metrics, as even though the network is approximately 26% less tolerant of random attacks and more centralized than the Cameron and Harris networks. The broad spatial distribution of available redundant paths in the Bexar network identified previously indicates critical substations are more difficult to disconnect from the rest of this network, owing to their global and local connectivity, and engineered design standards for network elements. Random attacks in contrast will often remove vital substations within the outer ring or inner small clusters connecting them, rapidly degrading network functionality. The total decline and rate of decline in performance metrics are also substantially less for the Bexar network at likely hurricane wind speeds. The Harris network performance is between that of the Bexar and Cameron networks in all metrics as well. While the absolute proportion of redundancy quantified by M appears to be lower in the Bexar network, the 26–85% greater local connectivity between nodes indicated by γ_G along with the substantially greater degree of centralization demonstrates that a majority of redundant paths in the Bexar network pass through several central nodes (yet non-dominant among themselves) compared to the other networks under consideration where very critical nodes are lone elements. The proportion of 4-cycles within the Bexar network is also 10–12% greater than the Cameron and Harris networks, though the latter network does contain a larger fraction of planar 3- and 5-cycles. A higher proportion of shorter planar cycles should correlate to increased reliability due to the decreased likelihood of edge or substation failure within such cycles, but the differences in network path length distributions are too small to evaluate the strength of this relationship. The clustering coefficient, which includes non-planar 3-cycles is deemed as an alternative metric as listed in Table 2.

The results in this section show that network hurricane performance can therefore be predicted using the selected metrics when coupled with the developed damage model. The ring–mesh topology of the Bexar network is demonstrated to maintain superior functionality when subject to severe hurricane hazards. The substation ring within the Bexar network, in addition to being heavily interconnected, contains many central substations that transmit power to smaller branches and cliques of substations throughout the county, thus reducing congestion. This topological arrangement of a highly redundant and well distributed substation set serving small, interconnected clusters through irregular meshes ensures that electrical service is maintained within the Bexar network until a substantial number of substations and transmission lines have failed. The design and retrofitting of transmission networks should strive to incorporate substation rings and increased connectivity within and across local scales to reduce flow bottlenecks and improve overall system reliability.

5. Conclusions

The developed power system performance model generates rapid assessments of distribution and transmission level network damage through the use of component fragility models. This model is readily applicable to practical power networks with only a minimum of required information. An application is shown-comparing the hurricane responses exhibited by topologically disparate networks. The spatial distribution of predicted damage is validated through the use of these models and a system topology synthesized from real transmission system data and the local road networks to approximate distribution level power systems. This approach results in an overall outage prediction model error of 15.59% and a standard error of 0.02%. Transmission network damage probabilities, accounting for topological features within the networks, are estimated through several network performance parameters such as LCC, abnormal betweenness distribution and loss, and the critical wind speed W_c parameter calculated for each network. Alternative methods to characterize resistance to disruptions, such as the critical fraction of removed nodes p_c parameter or simple betweenness from degree based targeted attacks, lack consideration for spatial factors that affect network component damage probability although they provide topological insights about the structure of the networks. As a result, traditional graph theoretic metrics cannot predict hurricane damage response alone due the lack of spatial dependence affecting network element fragility and failure. However, topological metrics coupled with damage models uniquely reveal the contribution of system layout to reliability.

Meshedness, clustering, and centralization are identified as critical topological factors that influence system reliability. Two distinct wind damage regimes arise from differences in these topological properties. Transmission networks similar to that of Cameron County, composed primarily of weakly interconnected hub nodes, cannot tolerate wind damage due to a lack of redundancy and long vulnerable links leading to a rapid decline in network function that occurs at lower wind speeds and more extensive performance decline compared to networks with more favorable topology. The compact irregular ring mesh topology of the Bexar network effectively reduces the loss of major network functionality due to the presence of a central substation ring that maintains service to dependent substations interconnected by shortcut links until substantial damage has been inflicted upon the network. This topology retains more functionality without congestion at all wind speeds and only begins to degrade rapidly at rare wind speeds above 58 m s^{-1}. The Harris network has a level of redundancy bounded by the Bexar and the Cameron networks with no single dominant topological feature; the performance rank of the network is appropriately between the two other networks.

Under topological and reliability considerations, the ring–mesh network topology provides superior performance when subject to hurricane hazards despite a suggested vulnerability to random failures given that a larger proportion of nodes actively contribute to overall network centrality and connectivity. Overall network reliability may be improved by introducing the previously identified substation rings into existing networks and by increasing the number of redundant short range links between central substations through paths that connect small clusters and reduce bottlenecks. The effect of modifications to improve system reliability can be easily tested for all levels of power transmission and distribution networks by observing the spatial damage distribution or rate of decline in network performance indicators, since network topology is connected directly to the hurricane damage response of a network. No other comparable model provides a link between network topology, spatial features, and system reliability to conduct such network performance studies. This work thus marks an advance in the evaluation of lifeline system reliability and performance prediction while providing a new tool for policy makers to assess the local impact of hurricanes on infrastructure and make recommendations for enhanced future performance as illustrated with electrical networks.

Several avenues of future study are required to broaden the applicability of these conclusions. Additional work is needed to determine the optimum topological properties for overall system reliability, design, and retrofit under operational and monetary constraints due to the many as yet unknown factors that influence performance when networks are subject to hazards or unknown failures and attacks—unknown failure causes still contribute significantly to the totality of events that trigger service interruption. Further analysis of topological compromises necessary to achieve hurricane damage tolerance versus resistance to random failures, system malfunctions, and other internal errors of networks is vital to avoid inadvertently creating vulnerabilities within power transmission networks to a specific failure type. Several authors have suggested that power transmission topologies favoring reliability under particular impacts may reduce network tolerance for other types of failures [28,66]; a comparative study of power transmission grids and corresponding artificial graphs is recommended to explore this possibility. The numerous causes of component failures must be investigated as well to ensure that all sources of network errors and failures are known when performing network reliability and loss of performance mitigation studies.

Acknowledgments

The authors of this paper gratefully acknowledge the support from the National Science Foundation through Grant CMMI 0728040 and the Shell Center for Sustainability at Rice University.

Table A1
Select introduced notation.

AE_z	Error in outage prediction for the z th ZIP code
$\widehat{B}$	Network centralization score
C_k^*	Normalized proportion of network k-cycles
$G(V,E)$	Power network with node set V and line (edge) set E
$\langle k \rangle$	Average substation degree
$\widehat{L}$	Average transmission line length (km)
$\widehat{ME}$	Average ZIP code outage prediction error
M	Normalized network meshedness
N	Number of Monte Carlo simulation model iterations
p_c	Critical fraction of randomly removed nodes from G
p_{LCC}	Largest connected cluster size estimates as a function of $\widehat{W}_s$.
$p_{pred,z}$	Predicted outage proportion for the z th ZIP code
$p_{act,z}$	Actual outage proportion for the z th ZIP code
$p_{f,i}$	Failure probability of element i
$p_{f,SS,i}$	Failure probability for the ith substation
$p_{f,LP,j}$	Failure probability for the jth distribution load point
$p_{f,TL,k}$	Failure probability of the kth transmission line
$p_{f,DL,k}$	Failure probability of the kth distribution line
$p_{f,FD}$	Failure probability of distribution lines due to flying debris impacts
V_{ss}	List of unique substations in a power network
V_p	List of nodes with greater than 90th percentile betweenness scores
W_s	Wind gust speed
$\widehat{W}_s$	Mean wind speed gust
W_c	Wind speed at which p_c node proportion is removed from G
Z	ZIP code count
α	Scaling factor to adjust substation abnormal current event tolerance
β	Scaling factor to adjust flying debris impact risk
γ	Scaling factor to adjust line breakage risk
γ_G	Graph clustering coefficient
σ_e	Standard error of developed damage model

Table A2
Power network components included in physical damage model.

Component	Purpose
Substation	Transmit power to other substations and distribution points
Distribution load point	Provide power to homes and businesses
Transmission line	Connect substations and power plants
Distribution line	Connect load points to substations

Table A3
Power system component fragility and hazard models.

Component	Model	Parameters	Source(s)
Substation	HAZUS-MH model 4735	Lognormal μ, σ	[67,68]
Distribution load point	Fragility curve	Lognormal μ, σ	[50]
Transmission line	Wind load model	$\gamma = 0.055$	[39,40]
Distribution line	Wind load model	$\gamma = 0.5$	[39,40]
Debris	Windthrow regression	$a_i, b_i, c_i; \alpha = 0.2$	[54]

Appendix A. Power network model, component, and fragility information

Select nomenclature is listed in Table A1. Power network components in the physical damage model are detailed in Table A2, and power system component fragility and hazard models are presented in Table A3.

Appendix B. Physical damage model algorithms

Algorithm B1. Component (element) fragility calculation.

Require $G(V,E), A_V, A_E$ {A_V, A_E are node/edge annotations (respectively)}
$P_V = \{\}$ {Array to record node failure probabilities}
$P_E = \{\}$ {Array to record edge failure probabilities}
for all $v \in V$ **do**
  $P_V(v) \Leftarrow FM(W(v), A(v))$ {FM: fragility model, $W(v)$: wind speed at node v, $A(v)$: annotations for poles and substations}
end for
for all $e \in E$ **do**
  $P_E(e) \Leftarrow FM(W(e), A(e))$ {FM: fragility model, $W(e)$: wind speed at edge e, $A(e)$: annotations for edges}
end for
return P_V, P_E

Algorithm B2. Fragility-based and disconnection damage model.

Require $G(V,E), V_{SS}, V_g$ {V_g: the set of generators}
$P_V, P_E \Leftarrow$ Algorithm B1
$O_V \leftarrow 0$ {Initialize abnormal current event count}
$F_V(v \in V) \leftarrow 0$ {Iinitial node states (0: active, 1:failed)}
$F_E(e \in E) \leftarrow 0$ {Initial edge states (0: active, 1:failed)}
$q \leftarrow 1$ {iteration number}
repeat
  $G_{old} \leftarrow G$ {Retain copy of undamaged network}
  for all $k \in G$ **do** {Generate failure distribution for current iteration }
    $r \Leftarrow rand()$ {$k \in K$ is either an edge (e) or a node (v) in G, yields $F_{V,q}, F_{E,q}$}
    if $r \leq P_K(k)$ **then**
      $F_{K,q}(k) \Leftarrow 1$
      Remove k from G
    end if
  end for
  repeat {Propagate node failures within the power network until a steady state is reached}
    $F_{V,old} = F_{V,q} \subset F_{K,q}$ {Store current node failure array to determine if the network has reached steady state}
    for all $v \in V$, **do**
      if $F_{v,q}$(neighbors of v) = **0**, $F_{v,q}(V_g)$=**0** or $V_g \bigcap C(v) = \emptyset$ **then**
        $F_{V,q}(v) = 1$ {Fail node v if isolated or is not connected to a generator in the cluster containing v ($C(v)$)}
      end if
    end for
    for all $v \in V$ **do**
      if $|\Delta C_B(v)| > \alpha$ **then** {$C_B(v)$: betweenness centrality of v}
        $O_{V_q}(v) = O_{V_q}(v) + 1$
      end if
    end for
  until [Cease looping if node failure vector is constant]$F_{V,old}$ is $F_{V,q}$
  $G \leftarrow G_{old}$ {Restore original network}
  $q \leftarrow q + 1$
until q is N
return [Return element response matrices (N column vectors) for further analysis] F_V, F_E, O_V

References

[1] Zhou Y, Pahwa A, Yang SS. Modeling weather-related failures of overhead distribution lines. IEEE Transactions on Power Systems 2006;21(4):1683–90.
[2] Brown RE, Gupta S, Christie RD, Venkata SS, Fletcher R. Distribution system reliability assessment: momentary interruptions and storms. IEEE Transactions on Power Delivery 1997;12(4):1569–75.
[3] Balijepalli N, Venkata SS, Christie RD. Modeling and analysis of distribution reliability indices. IEEE Transactions on Power Delivery 2004;19(4):1950–5.
[4] Reed DA. Electric utility distribution analysis for extreme winds. Journal of Wind Engineering & Industrial Aerodynamics 2008;96(1):123–40.
[5] Stillman RH. Probabilistic derivation of overstress for overhead distribution-line structures. IEEE Transactions on Reliability 1994;43(3):366–74.
[6] Stillman RH. Modeling failure data of overhead distribution systems. IEEE Transactions on Power Delivery 2000;15(4):1238–42.
[7] Radmer DT, Kuntz PA, Christie RD, Venkata SS, Fletcher RH. Predicting vegetation-related failure rates for overhead distribution feeders. IEEE Transactions on Power Delivery 2002;17(4):1170–5.
[8] Balijepalli N, Venkata SS, Richter Jr CW, Christie RD, Longo VJ, Mumbai I. Distribution system reliability assessment due to lightning storms. IEEE Transactions on Power Delivery 2005;20(3):2153–9.
[9] Hwang HHM, Chou T. Evaluation of seismic performance of an electric substation using event tree/fault tree technique. Probabilistic Engineering Mechanics 1998;13(2):117–24.
[10] Shinozuka M, Dong X, Chen TC, Jin X. Seismic performance of electric transmission network under component failures. Earthquake Engineering & Structural Dynamics 2007;36(2):227–44.
[11] Davidson RA, Haibin L, Sarpong IK, Sparks P, Rosowsky DV. Electric power distribution system performance in Carolina hurricanes. Natural Hazards Review 2003;4:36.
[12] Liu H, Davidson RA, Rosowsky DV, Stedinger JR. Negative binomial regression of electric power outages in hurricanes. Journal of Infrastructure Systems 2005;11:258.
[13] Han SR, Guikema SD, Quiring SM, Lee KH, Rosowsky D, Davidson RA. Estimating the spatial distribution of power outages during hurricanes in the Gulf Coast region. Reliability Engineering and System Safety 2009;94(2):199–210.
[14] Guikema SD, Goffelt JP. A flexible count data regression model for risk analysis. Risk Analysis 2008;28(1):213–23.
[15] Albert R, Albert I, Nakarado GL. Structural vulnerability of the North American power grid. Physical Review E 2004;69(2):025103–7.
[16] Crucitti P, Latora V, Marchiori M. A topological analysis of the Italian electric power grid. Physica A: Statistical Mechanics and its Applications 2004;338(1–2):92–7.

[17] Kinney R, Crucitti P, Albert R, Latora V. Modeling cascading failures in the North American power grid. The European Physical Journal B—Condensed Matter 2005;46(1):101–7.
[18] Chassin DP, Posse C. Evaluating North American electric grid reliability using the Barabasi–Albert network model. Physica A: Statistical Mechanics and its Applications 2005;355(2–4):667–77.
[19] Holmgren AJ. Using graph models to analyze the vulnerability of electric power networks. Risk Analysis 2006;26(4):955–69.
[20] Rosas-Casals MI, Valverde S, Solé RV. Topological vulnerability of the European power grid under errors and attacks. International Journal of Bifurcation and Chaos 2007;17(7):2465–75.
[21] Cardillo A, Scellato S, Latora V, Porta S. Structural properties of planar graphs of urban street patterns. Physical Review E 2006;73(6).
[22] Lämmer S, Gehlsen B, Helbing D. Scaling laws in the spatial structure of urban road networks. Physica A: Statistical Mechanics and its Applications 2006;363(1):89–95.
[23] Buzna L, Issacharoff L, Helbing D. The evolution of the topology of high-voltage electricity networks. International Journal of Critical Infrastructures 2009;5(1):72–85.
[24] Freeman LC. A set of measures of centrality based on betweenness. Sociometry 1977;40(1):35–41.
[25] Brandes U. A faster algorithm for betweenness centrality. Journal of Mathematical Sociology 2001;25(2):163–77.
[26] Dueñas-Osorio L, Vemuru SM. Cascading failures in complex infrastructure systems. Structural Safety 2009;31:157–67.
[27] Simonsen I, Buzna L, Peters K, Bornholdt S, Helbing D. Transient dynamics increasing network vulnerability to cascading failures. Physical Review Letters 2008;100(21):218701–9100.
[28] Rosas-Casals M, Corominas-Murtra B. Assessing European power grid reliability by means of topological measures. Transactions of the Wessex Institute 2000;121.
[29] Solé RV, Rosas-Casals M, Corominas-Murtra B, Valverde S. Robustness of the European power grids under intentional attack. Physical Review E 2008;77:026102.
[30] Diestel R. Graph theory. Berlin, Heidelberg: Springer; 2006.
[31] Platts. Topology of the State of Texas power transmission network; 2009. [accessed 05/2009] 〈http://www.platts.com/〉.
[32] Short TA. Electric power distribution handbook. Boca Raton: CRC Press; 2004.
[33] Texas Tech University, Harris County Road Network; 2009. [accessed 05/2009] 〈http://www.gis.ttu.edu/center/〉.
[34] Willis HL. Power distribution planning reference book. Boca Raton: CRC Press; 2004.
[35] Bollobas B. Modern graph theory. Berlin: Springer; 1998.
[36] Watts DJ. Small worlds: the dynamics of networks between order and randomness. Princeton: Princeton University Press; 2003.
[37] Newman MEJ. The structure and function of complex networks. SIAM Review 2003;45:167–256.
[38] Quanta Technology. Cost benefit analysis of the deployment utility infrastructure upgrades and storm hardening programs. Technical Report No. 36375 for the Public Utility Commission of Texas; 2009.
[39] American Society of Civil Engineers. Substation structure design guide (No. 113). ASCE manuals and reports on engineering practices; 2008.
[40] Bayliss CR, Hardy BJ. Transmission and distribution electrical engineering. London: Newnes; 2007.
[41] Multi-Resolution Land Characteristics Consortium. National land cover database; 2001 [accessed 05/2009] 〈www.mrlc.gov〉.
[42] Vickery PJ, Twisdale LA. Prediction of hurricane wind speeds in the United States. Journal of Structural Engineering 1995;121(11):1691–9.
[43] Vickery PJ, Lin J, Skerlj PF, Twisdale Jr. LA, Huang K. HAZUS-MH hurricane model methodology. I: hurricane hazard, terrain, and wind load modeling. Natural Hazards Review 2006;7:82.
[44] HURREVAC. Hurricane Ike Harris County Scenario, 2008 [accessed 03/2009] 〈ftp.hurrevac2.com/hurrevac.com/hurrdata/hurwin95/i_2008.stm〉.
[45] Georgiou PN. Design wind speeds in tropical cyclone-prone regions; 1987.
[46] Batts ME, Simiu E, Russell LR. Hurricane wind speeds in the United States. Journal of the Structural Division 1980;106(10):2001–16.
[47] Huang Z, Rosowsky DV, Sparks PR. Hurricane simulation techniques for the evaluation of wind-speeds and expected insurance losses. Journal of Wind Engineering & Industrial Aerodynamics 2001;89(7–8):605–17.
[48] Centerpoint Energy. Centerpoint energy Ike storm center; 2008 [accessed 03/2009] 〈www.centerpointenergy.com/newsroom/stormcenter/ike/〉.
[49] Personal Communication with Frank Lavelle concerning the extraction of HAZUS-MH fragility curves (Applied Research Associates); 2008.
[50] Gustavsen B, Rolfseng L. Asset management of wood pole utility structures. International Journal of Electrical Power and Energy Systems 2005;27(9–10):641–6.
[51] Oliver SE, Moriarty WW, Holmes JD. A risk model for design of transmission line systems against thunderstorm downburst winds. Engineering Structures 2000;22(9):1173–9.
[52] Holmes JD. Recent developments in the specification of wind loads on transmission lines. Journal of Wind & Engineering 2008;5(1):8–18.
[53] Milford RV, Goliger AM. Tornado risk model for transmission line design. Journal of Wind Engineering & Industrial Aerodynamics 1997;72:469–478.
[54] Canham CD, Papaik MJ, Latty EF. Interspecific variation in susceptibility to windthrow as a function of tree size and storm severity for northern temperate tree species. Canadian Journal of Forest Research 2001;31(1):1–10.
[55] Xi W, Peet RK, Decoster JK, Urban DL. Tree damage risk factors associated with large, infrequent wind disturbances of Carolina forests. Forestry 2008;81(3):317–34.
[56] Rich RL, Frelich LE, Reich PB. Wind-throw mortality in the southern boreal forest: effects of species, diameter and stand age. Journal of Ecology 2007;95(6):1261–73.
[57] Papaik MJ, Canham CD. Species resistance and community response to wind disturbance regimes in northern temperate forests. Journal of Ecology 2006;94(5):1011–26.
[58] Lanquaye-Opoku N, Mitchell SJ. Portability of stand-level empirical windthrow risk models. Forest Ecology and Management 2005;216(1–3):134–48.
[59] Gardiner B, Peltola H, Kellomäki S. Comparison of two models for predicting the critical wind speeds required to damage coniferous trees. Ecological Modelling 2000;129(1):1–23.
[60] Gardiner B, Byrne K, Hale S, Kamimura K, Mitchell SJ, Peltola H, et al. A review of mechanistic modelling of wind damage risk to forests. Forestry 2008;81(3):447–63.
[61] Duenas-Osorio L, Craig JI, Goodno BJ, Bostrom A. Interdependent response of networked systems. Journal of Infrastructure Systems 2007;13:185–194.
[62] Adachi T, Ellingwood BR. Serviceability of earthquake-damaged water systems: effects of electrical power availability and power backup systems on system vulnerability. Reliability Engineering and System Safety 2008;93(1):78–88.
[63] Cohen R, Erez K, ben Avraham D, Havlin S. Resilience of the internet to random breakdowns. Physical Review Letters 2000;85(21):4626.
[64] Alon N. Finding and counting given length cycles. Algorithmica 1997;17(3):209–23.
[65] Borgatti SP, Everett MG, Freeman LC. UCInet for Windows: software for social network analysis. Analytic Technologies; 2002.
[66] Pepyne DL. Topology and cascading line outages in power grids. Journal of Systems Science and Systems Engineering 2007;16(2):202–21.
[67] Vickery PJ, Skerlj PF, Lin J, Twisdale Jr. LA, Young MA, Lavelle FM. HAZUS-MH hurricane model methodology. II: damage and loss estimation. Natural Hazards Review 2006;7:94.
[68] Jain VK, Davidson R, Rosowsky D. Modeling changes in hurricane risk over time. Natural Hazards Review 2005;6:88–96.